The kinematics of the barred spiral galaxy NGC 3059

Bottema, R.

Published in:
Astronomy & astrophysics

Publication date:
1990

Astron. Astrophys. 233, 372–378 (1990)

ASTRONOMY
AND
ASTROPHYSICS

The kinematics of the barred spiral galaxy NGC 3059 *

R. Bottema

Kapteyn Astronomical Institute, University of Groningen, P.O. Box 800, NL-9700 AV Groningen, The Netherlands

Received July 12, accepted December 8, 1989

Abstract. Stellar and Hβ emission line radial velocities and stellar velocity dispersion measurements of the bar of the face-on SBc spiral galaxy NGC 3059 are presented. Along the major axis of the bar the radial velocities are constant, but going in a direction perpendicular to the bar from one side to the other, there is a substantial velocity increment of 70 km s^{-1}. Assuming that the systematic motions are confined to the plane of the galaxy, this jump can be explained by a stellar streaming of about 100 km s^{-1} along the bar, as predicted by numerical studies. The emission line radial velocities generally follow the stellar velocities with some small scale deviations. The stellar velocity dispersion is essentially constant at a level of 53 ± 5 km s^{-1} in the bar, and drops steeply outside. Comparison with z-direction bar dispersions of other galaxies shows that this value is considerably lower than the average value of ~ 140 km s^{-1} for SB0 galaxy bars.

Key words: galaxies: barred – kinematics and dynamics – structure of galaxies – NGC 3059

1. Introduction

As a part of an ongoing project to study the stellar velocity dispersion of galactic disks (van der Kruit and Freeman, 1984, 1986; Bottema et al., 1987; Bottema, 1988, 1989) absorption line spectra were taken of the small SBc galaxy NGC 3059. The close to face-on orientation should enable one to determine the perpendicular velocity dispersion of the disk as a function of radius. Unfortunately this proved impossible, both because the surface brightness of the disk and the velocity dispersion turned out to be very low. NGC 3059 has a small bar, about two magnitudes brighter than the surrounding disk and the observations did allow a clear determination of the stellar radial velocities and velocity dispersions in the bar region.

While theoretical studies of the dynamics of bars are abundant (Kormendy, 1983, and references therein), actual observations are quite rare. Velocity dispersion measurements have been done for the bars of a few bright SB0 galaxies (Kormendy, 1983; Jarvis et al., 1988) but never before for the bars of faint Sc galaxies. For the latter class of galaxies the bar kinematics can, of course, be determined with more certainty because there is no confusion with the bulge kinematics.

The spectroscopic observations, data reduction, and results of the observations are presented in Sects. 2, 3, and 4. Digitization of the image of NGC 3059 on the ESO-SRC-J plate catalog provided the photometry, to be discussed in Sect. 5. The results of numerical calculations concerning bars are compared with the kinematics of the bar of NGC 3059 in Sect. 6 and in Sect. 7 a comparison is made between the properties of this galaxy and that of other barred galaxies. Finally in Sect. 8 the results are summarized and a few suggestions for future research are presented. Table 1 summarizes all the relevant physical parameters of NGC 3059 and Fig. 1 shows an optical photograph of the galaxy.

2. Instrumental setup and observations

The spectroscopic observations of NGC 3059 were carried out from January 6 to 11, 1985 with the 3.6 m telescope at the European Southern Observatory, La Silla in Chile. At the Cassegrain focus the Boller and Chivens spectrograph was configured to produce a spectrum with a half power width resolution of about 1.5 Å ($=90$ km s^{-1}, consequently the resolution *dispersion* $=38$ km s^{-1}), around 5100 Å. The data were recorded on an RCA-CCD chip having a size of 512×320 pixels, 11 electrons per ADU (Analog Digital Unit), and a read-out noise of 3.5 ADU. The slit length of 3′ covered the range of 153 pixels so that the spatial length of 1 spectral row is 1″.18. The seeing during the observations ranged between two and three arcseconds and consequently always two to three spectral rows are correlated. Of the 512 pixels in the wavelength direction 500 were used ranging from 4842 to 5259 Å (417 Å) which after conversion to a velocity scale resulted in 49.55 km s^{-1} per pixel.

NGC 3059 was observed with two different orientations of the slit. An integration of 5^h57^m was made along the major axis of the bar (denoted as $\parallel$), and an integration of 6^h45^m was made perpendicular to the bar (denoted as $\perp$). For both integrations the centre of the galaxy was put at the centre of the slit and the extent of the galaxy was small enough to ensure that near both ends of the slit the sky spectrum could be observed simultaneously. The observations were divided up into single exposures of $1\frac{1}{2}$ to 2 hours, each preceded by an exposure to a He-Ar calibration lamp. Several template stars of spectral type close to K0III were observed, preceded by a calibration lamp exposure. At regular intervals zero second exposures were made to determine the bias level and read-out noise. A long dark integration was made to check the dark current and flat field images were recorded by observing an illuminated white sheet attached to the dome.

* Based on observations collected at the European Southern Observatory, La Silla, Chile

Table 1. Parameters of NGC 3059

R.A. (1950)	$9^h49^m41^s$	Shapley-Ames cat.
Declination (1950)	$-73°41'.2$	Shapley-Ames cat.
Hubble type	SBc(s) III	Shapley-Ames cat.
B_T	12.03	Shapley-Ames cat.
Systemic velocity	$1245 \pm 5\,km\,s^{-1}$	This study
Pos. angle bar	39°	This study
Phot. scalelength	32".8	This study
Extrapol. central surface brightness	$21.39 \pm 0.25\,J\,mag\,arcsec^{-2}$	This study
Distance	13.2 Mpc	Adopted

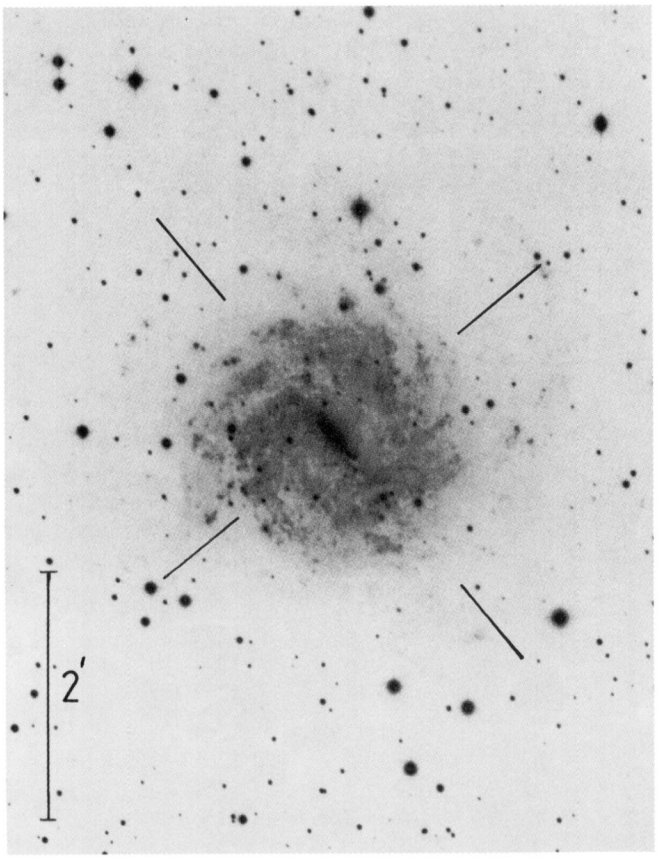

Fig. 1. Reproduction of the image of NGC 3059 from page 107 of the Revised Shapley-Ames catalogue (Sandage and Tammann, 1981). The galaxy was observed with the 3' long spectrograph slit positioned along the major axis of the bar (p.a. 39°) and in a position perpendicular to the bar (p.a. 129°), as indicated. North at top, East at left

Unfortunately there were about 20 skylines in the spectrum that originated from infrared straylight of the first order spectrum of the same grating. Also the flat field exposures suffered from infrared contamination. Hence these flat fields could not be used to correct for the pixel-to-pixel response but still were useful to largely correct for the large scale response of the chip. It turned out that the faint skylines could be properly subtracted but about five bright lines were so completely dominating the spectrum that at those wavelengths the spectrum could not be used. Before cross-correlation and after continuum subtraction these regions were set to zero and so did not enter in the cross-correlation sum.

3. Data reduction

The total data reduction proceeded along the standard lines. First, the bias level was subtracted from all of the images. The dark current amounted to less than 2 ADU's in one hour, so no correction was made for this. The effect of cosmic rays was removed by comparing two spectral images of the same object, at the positions where the spectra differed substantially data were removed and replaced by the interpolated value of the surrounding pixels. The pollution by cosmic rays turned out to be approximately 1% of the chip for one hour integration. A correction for the large scale response of the chip was made by dividing the images by a normalized and strongly smoothed flat field exposure.

For the wavelength calibration ~12 lines were used evenly spaced over the 417 Å interval, a second order polynomial was fitted in the wavelength direction and a third order in the slit direction. The standard deviation of the 12 lines from the wavelength solution was never larger than $5\,km\,s^{-1}$. Then the exposures were regridded to a log λ scale with $49.55\,km\,s^{-1}$ per pixel. The images were added and subsequently the sky, determined by averaging a region at both ends of the slit, was subtracted. In this way two essentially clean spectra, one taken along the bar and one perpendicular to it, were constructed. The average number of ADU's as a function of position along the slit is shown in Fig. 2; this gives an impression of the countlevels involved. To all the spectral rows a low order polynomial was fitted which determined the continuum level. This level was subtracted, thus rejecting the line strength information but ensuring that at the faint levels where the continuum is ill defined the spectrum does not suffer from division by a very small number.

The stellar spectra were bias subtracted, calibrated in wavelength, regridded to a log λ scale and then shifted to one common redshift. Two essentially noise free template spectra were constructed by twice averaging half of the stellar spectra. As for the galaxy, the continuum was removed by fitting a polynomial to the spectrum and subtracting this from the data.

In order to achieve a sufficient signal-to-noise, spectra of the galaxy were added along the slit until a level around 150 ADU's or more was reached. For the observation along the major axis of the bar this averaging was done in two ways, first from side to side along the slit and secondly by starting at the position of maximum intensity and averaging spectra at equal distances around this central position. To determine the stellar kinematics the low frequency continuum and high frequency noise wavenumbers were filtered out. Regions heavily contaminated with skyline remnants or dominated by emission lines were revalued to the average spectral value and then the cross-correlation was perfor-

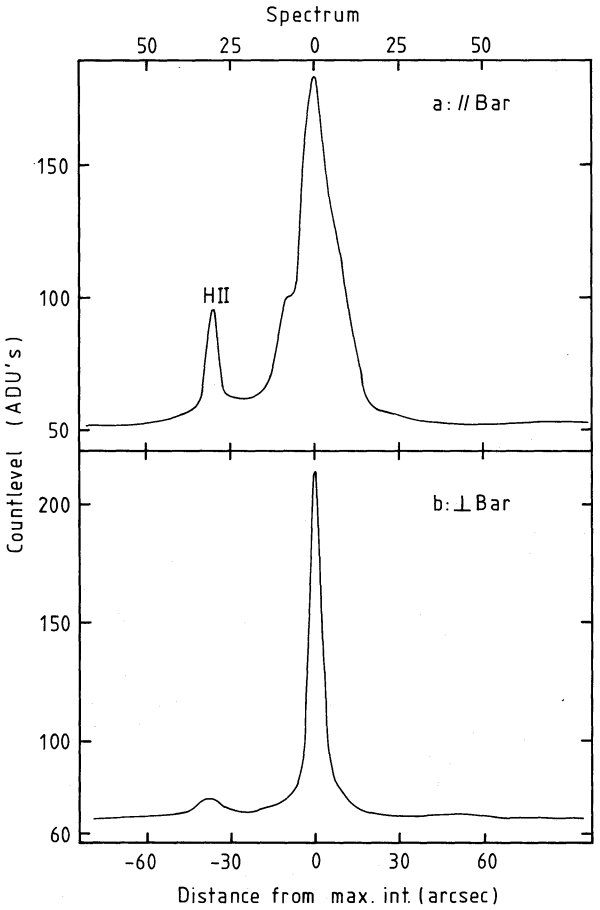

Fig. 2a and b. The countlevel along the slit, averaged over the observed wavelength extent, in analog digital units. The skyspectrum has not yet been subtracted. **a** For the slit ‖ to the bar. **b** For the slit ⊥ to the bar

med with the template spectra using standard Fourier techniques (Brault and White, 1971; Simkin, 1974; Tonry and Davis, 1979).

4. Results of the spectroscopic observations

The spectra revealed the very clear presence of strong Hβ emission in the bar region and the H II regions in the disk. The emission of the [O III] lines was a factor 4 to 5 weaker. Gaussians were fitted to the Hβ line profiles giving the radial velocities of the ionized gas. The numerical values are presented in Table 2, while Fig. 3 shows the velocities as a function of position along the slit.

The stellar kinematics follows from the cross-correlation procedure. It turned out that the difference between the kinematical values resulting from the use of the two different template spectra was at most 2 km s^{-1}. Compared with the intrinsic calibration error of about 5 km s^{-1} this difference is negligible. Hence only the results for the use of one template spectrum are presented.

The cc peaks which emerged give the stellar redshift and velocity dispersion by measuring their position and width respectively. The position is determined by fitting parabolas to the peaks over 3, 5, and 7 velocity bins and averaging the maxima. A fit in a least squares sense of model cc peaks to the observed data gives the velocity dispersion. The model cc peaks are constructed by convolving the template spectrum with known gaussian broadening functions. This procedure is documented in detail in Bottema (1988) and will not be described here. For the observations ‖ to the bar the observed and best fitting model peaks are shown in Fig. 4. An eye estimate of the dispersion error was made after projecting the model curves 20 or 30 km s^{-1} from the best fit on top of the data. It was judged that the spectral resolution does not allow the determination of dispersions smaller than 40 km s^{-1}.

Table 3 gives the radial velocities and dispersion values. Figure 3 shows the stellar velocities together with the emission line radial velocities as a function of position along the slit. Along the bar (‖)

Table 2. Hβ radial velocities

	Spectral row(s)	Dist. from max. int. (arcsec)	Helioc. radial vel. (km s^{-1})	Error (km s^{-1})
‖ bar	−34	−40.1	1211	7
	−33	−38.9	1209	6
	−32	−37.8	1212	5
	−31	−36.6	1212	5
	−30	−35.4	1209	6
	−29	−34.2	1202	7
	−10	−11.8	1222	5
	− 9	−10.6	1224	5
	− 8	− 9.4	1227	5
	− 7	− 8.3	1234	5
	− 6	− 7.1	1250	5
	− 5	− 5.9	1252	5
	− 4	− 4.7	1242	5
	− 3	− 3.5	1228	5
	− 2	− 2.4	1222	5
	− 1	− 1.2	1234	5
	0	0	1248	5
	1	1.2	1259	5
	2	2.4	1260	5
	3	3.5	1258	5
	4	4.7	1255	5
	5	5.9	1249	5
	6	7.1	1248	5
	7	8.3	1249	5
	8	9.4	1250	5
	9	10.6	1250	5
	10	11.8	1251	5
	11	13.0	1254	5
	12	14.2	1257	8
⊥ bar	−55: −45	−58.4	1292	7
	−44: −35	−46.6	1294	10
	−34: −25	−34.8	1299	7
	− 4	− 4.7	1265	7
	− 3	− 3.5	1265	6
	− 2	− 2.4	1261	5
	− 1	− 1.2	1256	5
	0	0	1230	5
	1	1.2	1221	5
	2	2.4	1219	5
	3	3.5	1224	7
	4	4.7	1231	8

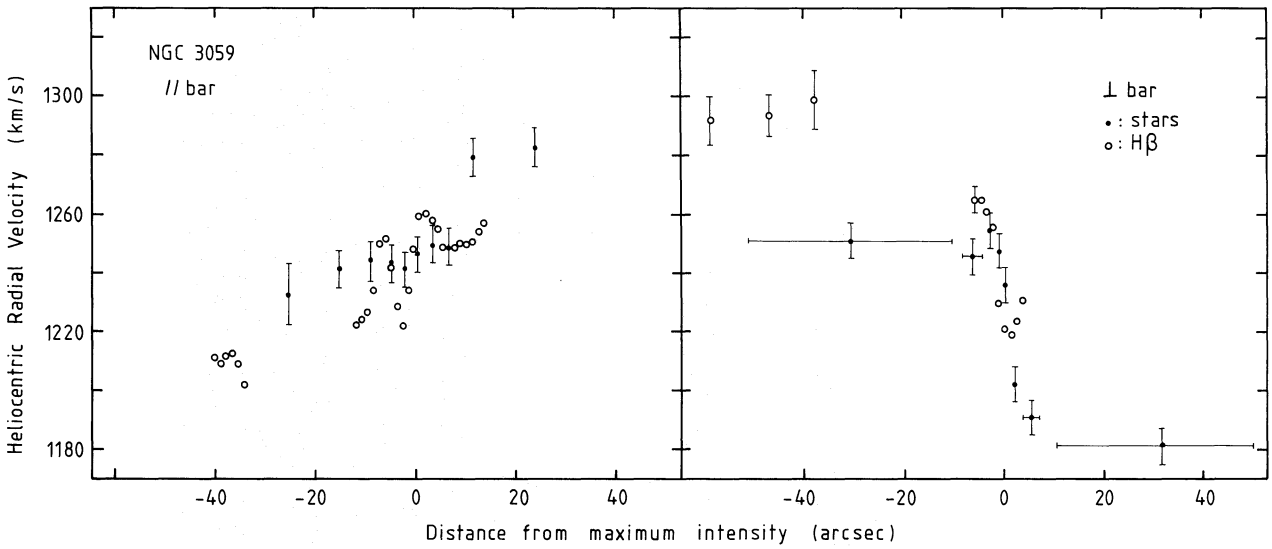

Fig. 3. The stellar and Hβ radial velocities determined for the two slit orientations. Note the considerable velocity jump (in the $\perp$ direction) when crossing the bar

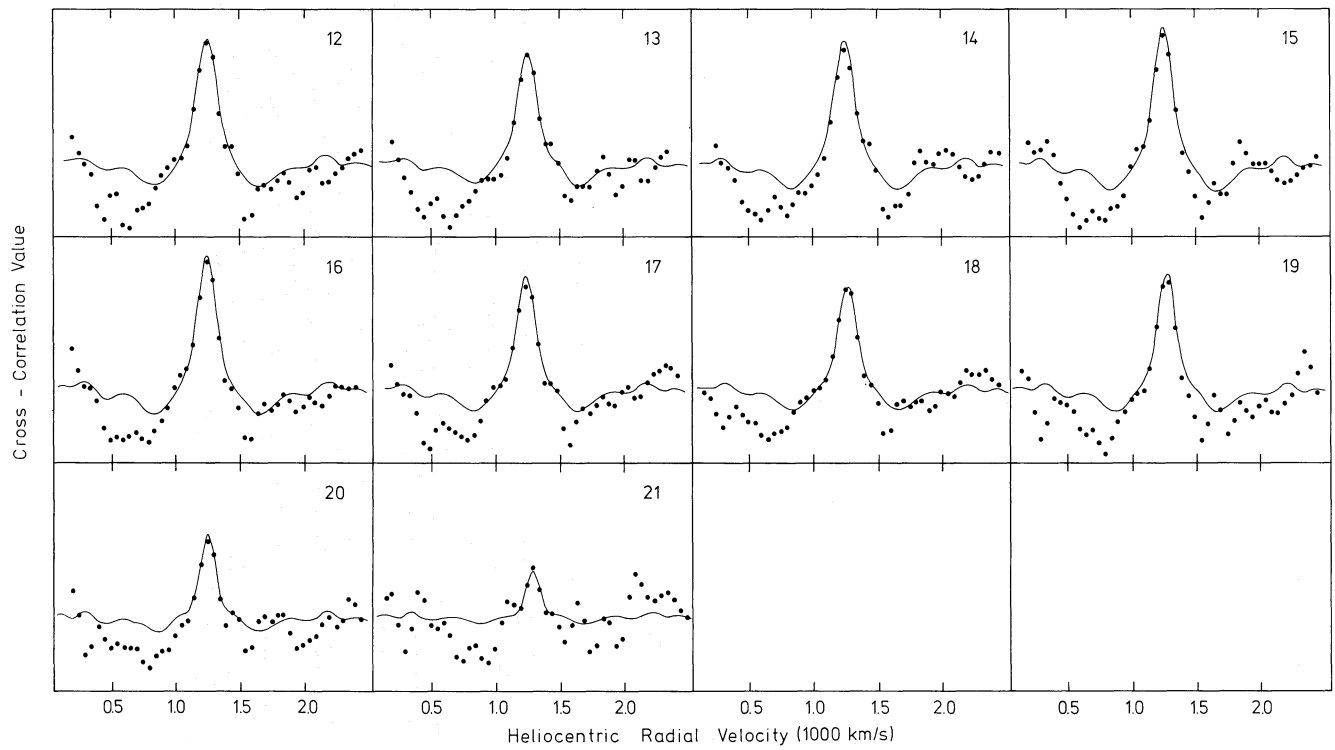

Fig. 4. The observed cross-correlation peaks (dots) with the best fitting model cross-correlation function superposed. The numbers in the top-right correspond to the numbers in Table 3. No meaningful physical value can be assigned to the cross-correlation value because the continuum has been subtracted

the stars have a nearly constant radial velocity around 1245 km s^{-1}, but going from one side of the bar to the other ($\perp$), there is a considerable velocity jump of 70 km s^{-1}. The Hβ velocities follow the stellar velocities on the large scale but on smaller scales the gas shows some rapid velocity changes. In Figs. 5 and 6 the velocity dispersion $\parallel$ to the bar and $\perp$ to the bar are shown respectively. It is evident that the perpendicular (or z-direction) velocity dispersion of the bar is constant at a level of 53 ± 5 km s^{-1} and that for radii outside the bar region the dispersion drops steeply to below the resolution limit.

5. Photometry

A photograph of NGC 3059 is depicted in Fig. 1, it is a reproduction of the image of the galaxy on page 107 of the revised Shapley-Ames (Sandage and Tammann, 1981) catalogue. It is a beautiful and clear example of an SBc galaxy which is almost perfectly oriented face-on. Due to the limited dynamical range of photographic emulsions the strength of the bar is very much disguised.

To determine the large scale properties of NGC 3059, the image of the galaxy on the ESO-SRC-J plate no. 037 was digitized.

Table 3. Stellar kinematics of NGC 3059

	No.	Averaged spectral rows	Dist. from max. int. (arcsec)	Helioc. radial vel. ($km\,s^{-1}$)	Velocity dispersion ($km\,s^{-1}$)	Dispersion error ($km\,s^{-1}$)
A) ∥ bar (1)	1	−31:−27	−34.2	1147	53	25
	2	−26:−17	−25.4	1232	–	–
	3	−16:−10	−15.3	1241	38	20
	4	− 9:−6	− 8.9	1244	61	10
	5	− 5:−3	− 4.7	1243	58	10
	6	− 2:−1	− 1.8	1242	56	10
	7	0:1	0.6	1246	58	10
	8	2:4	3.5	1249	46	10
	9	5:7	7.1	1248	40	15
	10	8:12	11.8	1279	46	10
	11	13:28	24.2	1282	–	–
B) ∥ bar (2)	12	0	0	1243	62	10
	13	− 1,1	1.2	1245	54	10
	14	− 2,2	2.4	1246	58	10
	15	− 3,3	3.5	1245	55	10
	16	− 5:−4,4:5	5.3	1245	52	10
	17	− 7:−6,6:7	7.7	1246	53	10
	18	− 9:−8,8:9	10.0	1254	55	10
	19	−12:−10,10:12	13.0	1270	48	15
	20	−18:−13,13:18	18.3	1244	35	20
	21	−39:−19,19:39	34.2	1287	<30	–
C) ⊥ bar	22	−44:−7	−30.1	1251	<30	–
	23	− 6:−3	− 5.3	1246	33	+10/−30
	24	− 2:−1	− 1.8	1255	60	10
	25	0	0	1248	42	10
	26	1	1.2	1236	50	10
	27	2:3	3.0	1202	57	15
	28	4:7	6.5	1191	44	15
	29	8:47	32.5	1181	–	–

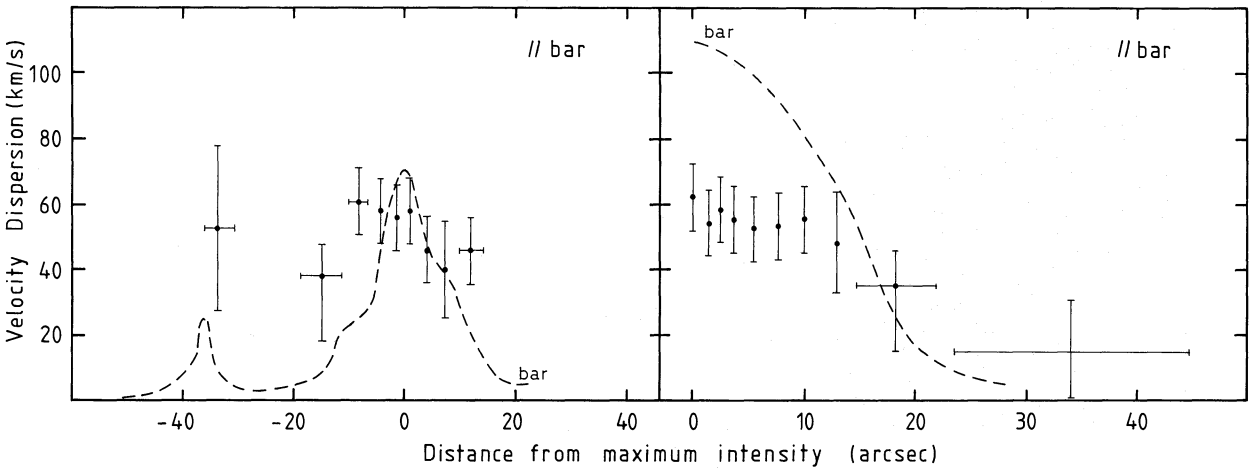

Fig. 5. The stellar velocity dispersions in the direction along the major axis of the bar. The surface brightness of the bar has been indicated by the dashed line

After calibration and skysubtraction an exponential disk fit was made to the region outside the bar out to a radius of 160″. The scalelength turned out to be 32″.8 (=2.1 kpc) and the disk has an extrapolated central surface brightness of 21.39 ± 0.25 J-mag arcsec^{-2}. The bar is on average about two magnitudes brighter than the disk in which it is embedded and the ratio of short to long bar axis amounts to 1:3.0.

To determine the inclination of the disk the ellipticity of a few isophotes, well outside the bar region, has been measured. The short to long axis ratio of the individual isophotes was generally

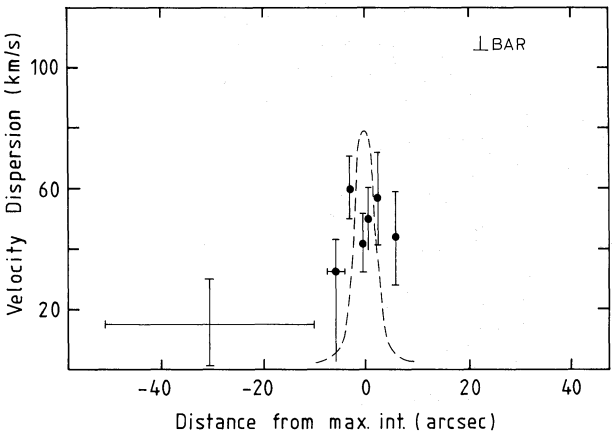

Fig. 6. As Fig. 5, but now in the direction ⊥ to the bar

larger than 0.93, but the position angles of the individual long axes differed substantially, covering a range between 25° and 90°. Hence the position angle of the major axis of NGC 3059 is ill defined while the inclination is certainly less than 20°.

Aperture photometry by Longo and de Vaucouleurs (1983) shows that the disk has a $B-V$ colour around 0.7, being quite typical for Sc galaxies. At smaller radii the galaxy is bluer, $B-V \sim 0.5$, indicating that in the central bar region a substantial star formation is going on. This was of course already indicated by the strong Hβ emission of the bar.

6. Comparison with numerical results

There have been many theoretical studies of barred galaxies, but the only selfconsistent models so far are produced by N-body simulations. In general bars appear naturally in a rotating stellar disk whenever the velocity dispersion is low. A low dispersion can be created by a cooling mechanism like continuous or recent star formation (Sellwood and Carlberg, 1984). Kormendy (1983) made a detailed comparison between the stellar kinematics of the SB0 galaxy NGC 936 and the results of numerical bar calculations by Miller and Smith (1979) and by Hohl and Zang (1979). Maps of stellar streaming produced by these authors clearly indicate that there is a substantial non-circular streaming along the bar. Theoretical studies (Teuben and Sanders, 1985; van Albada and Sanders, 1982) attribute this streaming along the bar to a family of stable stellar orbits which are highly elongated, roughly elliptical, and oriented along the long bar axis. At present, theoretical and numerical studies employ barred galaxy models where the systematic motions are confined to the plane of the galaxy disk. Such models can explain all bar phenomena very satisfactorily, both in two-dimensional calculations (Athanassoula and Sellwood, 1986; Sparke and Sellwood, 1987; Sellwood and Sparke, 1988) and in three dimensions (James and Sellwood, 1978; Combes and Sanders, 1981). Therefore in the following discussion it will be assumed that in the case of NGC 3059 also all systematic motions are in the plane of the galaxy.

For NGC 3059 a detailed comparison with numerical results is not possible because there is no information about the exact orientation of the galactic disk. Still, some qualitative conclusions can be drawn. It is obvious from Fig. 3 that along the bar the radial velocity is about constant but that along a line perpendicular to the bar there is a huge velocity jump of about 70 km s^{-1}. Even if the minor axis were lying along the bar (and so the major axis ⊥ to the bar) such a velocity jump over ~ half a photometric scalelength for an ScIII galaxy would only be possible if the galaxy is close to edge-on. Clearly for NGC 3059 this is not the case. To be a little more quantitative, the Tully-Fisher relation gives for NGC 3059 a maximum rotation velocity of 135 km s^{-1} (see Rubin et al., 1985 for $M_B \leftrightarrow V_{max}$ relation). For a bulge-less Sc type a pure disk rotation curve can be assumed (Freeman, 1970) reaching its maximum rotation around 2 photometric scalelengths ($2h$). Going from $R=0$ to $R=\frac{1}{4}h$ the rotation reaches ~40 km s^{-1}, so over the bar thickness the velocity range should be twice this value: 80 km s^{-1}. For an inclination $<20°$ the maximum jump in rotation is 22 km s^{-1}, far less than the observed jump of 70 km s^{-1}. So obviously almost the whole observed velocity jump must be due to a strong streaming along the bar. A lower limit of 100 km s^{-1} is given for $i<20°$. Thus the observations presented here are in good agreement with a substantial non-circular streaming along the bar as predicted by theory and numerical experiments.

A fact which should be noted is that for the spectrum taken along the major axis of the bar the gas shows a considerable change in radial velocity, much larger than for the stars. It appears that near the centre of the bar there is a strong radial inwards or outwards motion of the gas, or a substantial gas rotation. Whether or not this is consistent with theoretical expectations is not clear.

7. Comparison with other barred galaxies

At present, the velocity dispersion has been determined observationally for only a few barred galaxies; for example the work by Kormendy (1983) on the moderately inclined galaxy NGC 936 noted above. Because of its inclination the velocity dispersions in the R, Θ and z-directions cannot be disentangled and hence it is difficult to compare these data with the almost pure z-direction dispersion measured for NGC 3059. In a recent article by Jarvis et al. (1988) velocity dispersion data are presented for five close to face-on SB0 galaxies. For all the galaxies spectra were taken for two slit orientations, one along the major and one along the minor axis. Because these galaxies are nearly face-on the dispersion in the perpendicular direction will dominate. The morphological type (SB0), however, differs substantially from the type of NGC 3059. Moreover, all the observed galaxies have large bulges which makes it difficult to disentangle the bar and bulge dispersions.

It is difficult to estimate the true maximum rotation velocity in nearly face-on galaxies. This complicates a comparison of velocity dispersion with rotational velocity in such systems. To circumvent this problem the maximum rotational velocity may be estimated from the luminosity by using the Tully-Fisher relation for the appropriate morphological type (Rubin et al., 1985). For NGC 3059 the $M_B \leftrightarrow v_{max}$ curve for Sc galaxies was used and for the SB0 galaxies of the Jarvis et al. study, the curve for Sa type galaxies. The bar dispersion was determined by averaging the observed values at those radii where the photometry shows a plateau in the luminosity profile. In Table 4 the values for M_B, v_{max} and the z-bar dispersion are given. These values are of course only an estimate and are not intended to represent a precise measurement. Figure 7 shows the relation between maximum rotational velocity and bar z-velocity dispersion. It is clear that the larger galaxies also have a larger bar velocity dispersion. An explanation for this fact may be found by examining Fig. 2 of the paper by Athanassoula and Sellwood (1986). They give the growth rate of a bar mode as a function of disc mass fraction of the galaxy

Table 4. Bar z-velocity dispersion versus max. rotational velocity

Galaxy	M_B ($H_0=50$) (mag)	v_{max} (km s^{-1})	bar z-dispersion (km s^{-1})
NGC 3059	−20.14	135	53± 5
NGC 1291	−21.68	310	160±15
NGC 1543	−20.49	238	145±20
NGC 1574	−19.60	193	120±20
NGC 4477	−20.46	236	160±20
NGC 4754	−20.29	227	135±20

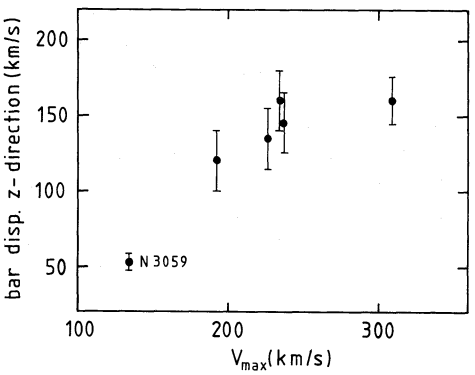

Fig. 7. The perpendicular (or z-direction) stellar velocity dispersion of the bar as a function of maximum rotational velocity. The result for NGC 3059 is compared with the bar dispersions of the SB0 galaxies in the Jarvis et al. (1988) study. The values shown are also tabulated in Table 4

(q) and stellar velocity dispersion divided by rotational velocity ($\langle v^2\rangle^{1/2}/v_{rot}$). Determined is a linear relation between growth rate and $\langle v^2\rangle^{1/2}/v_{rot}$ which shows that smaller galaxies will develop bars in a situation where the dispersion is lower. The bar dispersion is very likely to bear a close resemblance to the dispersion of the galaxy in which it developed and hence a larger bar dispersion will occur in larger galaxies. It turns out that the data in Fig. 7 are consistent with the results of Athanassoula and Sellwood.

8. Conclusions and suggestions for future work

The spectroscopic observations of the almost face-on SBc spiral NGC 3059 reveal that:

1. In a direction perpendicular to the bar there is a large velocity increment of 70 km s^{-1} from one side of the bar to the other. Assuming that the systematic motions are confined to the plane of the galaxy, this jump can be explained by a substantial stellar streaming of about 100 km s^{-1} along the bar.
2. This strong streaming along the bar agrees with the results of numerical calculations concerning barred galaxies.
3. The emission line radial velocities generally follow the stellar velocities with some small scale deviations.
4. The stellar velocity dispersion is constant in the bar at a level of 53±5 km s^{-1}, and drops steeply outside.
5. Comparison with z-direction bar dispersions of other galaxies shows that this value is considerably lower than the average value of ~140 km s^{-1} for SB0 galaxy bars.

Suggestions for future research:

a) An extensive spectroscopic observation of a barred Sc galaxy. This would enable the construction of a combined emission line and stellar velocity field. Comparison of the emission line and stellar kinematics will give insight into the form and magnitude of the underlying gravitational field.

b) The determination of the stellar velocity dispersion as a function of radius in a barred Sc galaxy inside and outside the bar. To this aim a spectroscopic setup with a resolution around 20 km s^{-1} should be used. The results could be compared with the velocity dispersions in unbarred galaxies.

c) The study of a number of Sc galaxy bars to determine the velocity dispersion of the bar as a function of galaxy mass.

Acknowledgements. The author wishes to thank the Netherlands Foundation for Radio Astronomy for letting him use their computer facilities to reduce the data. I also thank A. Pickles for introducing me to the software package Pandora, P. van der Kruit for digitizing the plate image of NGC 3059 and R. Sanders for valuable comments on the manuscript.

References

Albada, T.S. van, Sanders, R.H.: 1982, *Monthly Notices Roy. Astron. Soc.* **201**, 303
Athanassoula, E., Sellwood, J.A.: 1986, *Monthly Notices Roy. Astron. Soc.* **221**, 213
Bottema, R.: 1988, *Astron. Astrophys.* **197**, 105
Bottema, R.: 1989, *Astron. Astrophys.* **221**, 236
Bottema, R., Kruit, P.C. van der, Freeman, K.C.: 1987, *Astron. Astrophys.* **178**, 77
Brault, J.W., White, O.R.: 1971, *Astron. Astrophys.* **13**, 169
Combes, F., Sanders, R.H.: 1981, *Astron. Astrophys.* **96**, 164
Freeman, K.C.: 1970, *Astrophys. J.* **160**, 811
Hohl, F., Zang, T.A.: 1979, *Astron. J.* **84**, 585
James, R.A., Sellwood, J.A.: 1978, *Monthly Notices Roy. Astron. Soc.* **182**, 331
Jarvis, B.J., Dubath, P., Martinet, L., Bacon, R.: 1988, *Astron. Astrophys. Suppl.* **74**, 513
Kormendy, J.: 1983, *Astrophys. J.* **275**, 529
Kruit, P.C. van der, Freeman, K.C.: 1984, *Astrophys. J.* **278**, 81
Kruit, P.C. van der, Freeman, K.C.: 1986, *Astrophys. J.* **303**, 556
Longo, G., de Vaucouleurs, A.: 1983, *A General Catalogue of Photoelectric Magnitudes and Colors in the U, B, V system of 3578 Galaxies Brighter than the 16th Magnitude*, University of Texas Monographs in Astronomy, No. 3
Miller, R.H., Smith, B.F.: 1979, *Astrophys. J.* **227**, 785
Rubin, V.C., Burstein, D., Ford, W.K., Thonnard, N.: 1985, *Astrophys. J.* **289**, 81
Sandage, A., Tammann, G.A.: 1981, *A Revised Shapley-Ames Catalog of Bright Galaxies*, Carnegie Institute of Washington
Sellwood, J.A., Carlberg, R.G.: 1984, *Astrophys. J.* **282**, 61
Sellwood, J.A., Sparke, L.S.: 1988, *Monthly Notices Roy. Astron. Soc.* **231**, 25p
Simkin, S.M.: 1974, *Astron. Astrophys.* **31**, 129
Sparke, L.S., Sellwood, J.A.: 1987, *Monthly Notices Roy. Astron. Soc.* **225**, 653
Teuben, P.J., Sanders, R.H.: 1985, *Monthly Notices Roy. Astron. Soc.* **212**, 257
Tonry, J., Davis, M.: 1979, *Astron. J.* **84**, 1511